Carbohydrate Polymers 88 (2012) 882–890

Contents lists available at SciVerse ScienceDirect

Carbohydrate Polymers

journal homepage: www.elsevier.com/locate/carbpol

Structural characterization of cell wall pectin fractions in ripe strawberry fruits using AFM

Sara Posé [a], Andrew R. Kirby [c], José A. Mercado [b], Victor J. Morris [c], Miguel A. Quesada [a,*]

[a] Departamento de Biología Vegetal, Universidad de Málaga, Campus de Teatinos, 29071 Málaga, Spain
[b] Instituto de Hortofruticultura Subtropical y Mediterránea "La Mayora" (IHSM-UMA-CSIC), Departamento de Biología Vegetal, Universidad de Málaga, 29071 Málaga, Spain
[c] Institute of Food Research, Norwich Research Park, Colney, Norwich NR4 7UA, UK

ARTICLE INFO

Article history:
Received 14 November 2011
Received in revised form 8 January 2012
Accepted 9 January 2012
Available online 24 January 2012

Keywords:
Fragaria × *ananassa*
Fruit ripening
Fruit softening
Pectins
Primary cell wall
Atomic force microscopy

ABSTRACT

Cell wall disassembly during fruit ripening is the main process leading to fruit softening. In strawberry fruit (*Fragaria* × *ananassa*, Duch.), functional analysis with transgenic plants have related the loss of firm texture to the metabolism of pectins. To gain insights into the role of pectins in strawberry softening we have analyzed physicochemical features of ionic and covalently bound pectins, isolated from ripe fruits, by Fourier transform infrared spectroscopy (FTIR), size exclusion chromatography (SEC) and atomic force microscopy (AFM). Cell wall material was isolated and chemically fractionated by sequential extraction with cyclohexane-trans-l,2-diamine tetraacetate (CDTA) and sodium carbonate (Na_2CO_3) in order to extract ionic and covalently bound pectins, respectively. Uronic acids (UA) were detected as the main component in CDTA samples, whilst a significantly higher content of neutral sugar was observed in the Na_2CO_3 samples, representing 33% of total sugars vs. 12% in the CDTA fraction. The spectral profile in the FTIR region 1200–900 cm^{-1} was similar in the case of both pectin fractions, although some minor changes in the band intensities suggest an enrichment of the carbonate fraction in rhamnogalacturonan-I pectin domains. SEC analysis showed that the average molecular weight of the CDTA pectin was higher than that of the carbonate extract. AFM histograms of polymer length were well approximated by a Log normal distribution function for both pectin fractions. The CDTA and Na_2CO_3 polymer length distributions were statistically different with mean values of ~87 and 65 nm, respectively. AFM studies revealed the presence of sidechains and multiple branching, previously attributed to branching of the galacturonic acid backbone. Both fractions were about 9% branched, but the Na_2CO_3 samples showed a higher percentage of multi-branched polymers. These results demonstrate that AFM is an excellent tool revealing new information on pectin structure which, when combined with classical techniques such as FTIR or SEC, provides a deeper characterization of fruit pectins.

1. Introduction

Pectin is considered as one of the most complex natural plant biopolymers (Vincken et al., 2003; Voragen, Coenen, Verhoef, & Schols, 2009) although individual components are well characterized, the way they are interconnected structurally within the cell wall and in extracts is still not well understood. These polysaccharides are a major component of the primary cell wall of non-graminaceous plants, accounting for up to 60% of the cell wall mass in many fruits (Redgwell et al., 1997a). Pectin metabolism during fruit ripening is one of the key processes leading to a reduction in fruit firmness. Extracted pectins are also widely used as gelling agents and stabilisers in processed food products (Willats et al., 2006). Thus, a comprehension of the relationship between pectin structure and texture is essential for both plant and food scientists. Previous work by the authors has been focused on the role of cell wall disassembly in strawberry fruit softening. By means of a functional approach, we have shown how the changes in different pectin fractions are related to softening during strawberry ripening (Quesada et al., 2009; Santiago-Doménech et al., 2008).

The main component of pectin is D-galacturonic acid (GalA) and one of the major pectic component polysaccharides is homogalacturonan (HG), an essentially linear polymer consisting of (1→4) linked α-D GalA units with some of the carboxyl groups methyl-esterified or acetylated. The polygalacturonic (PGA) chain is interrupted by a pectic domain named Rhamnogalacturonan I (RGI) which is enriched in rhamnose (Rha) residues. RGI consists of

Abbreviations: AFM, atomic force microscopy; CDTA, cyclohexane-trans-l,2-diamine tetraacetate; FTIR, Fourier transform infrared spectroscopy; GalA, galacturonic acid; HG, homogalacturonan; L_N, number-average contour length; L_W, weight-average contour length; PDI, polydispersity index; PGA, polygalacturonic acid; RGI, rhamnogalacturonan I; RGII, rhamnogalacturonan II; SEC, size exclusion chromatography; UA, uronic acids.

* Corresponding author. Tel.: +34 952 13 4133.
E-mail address: quefe@uma.es (M.A. Quesada).

0144-8617/$ – see front matter © 2012 Elsevier Ltd. All rights reserved.
doi:10.1016/j.carbpol.2012.01.029

the repeating disaccharide [→4)-α-D-GalA-(1→2)-α-L-Rha-(1→] backbone decorated with neutral sugar sidechains. The composition of the RGI regions depends on plant source and extraction but may contain galactan, arabinan and/or arabinogalactan sidechains attached to the RGI backbone via Rha residues, forming highly branched (hairy) regions (Mohnen et al., 1996; Willats, McCartney, Mackie, & Knox, 2001). However, Vincken et al. (2003) have recently proposed an alternative structure to the above contigous structure in which the RGI form the backbone with HG regions attached as long side chains. The third type of pectic domain is Rhamnogalacturonan II (RG II), which is less abundant but very highly conserved in the plant kingdom, with a HG backbone and very complex side chains attached to the GalA residues (Willats et al., 2006).

As stated previously, pectins are extremely complex and their composition and structure vary with source species, tissues, environmental conditions and developmental stages. Cell wall disassembly during fruit ripening is a paradigmatic example of fast changes in different structural components, including pectic polymers, which result in a different fruit texture. In the case of strawberry fruits, this process is characterized by a high solubilisation of pectins (Figueroa et al., 2010; Redgwell et al., 1997a; Santiago-Doménech et al., 2008), a slight depolymerization of covalently bound pectins (Redgwell et al., 1997a; Rose, Hadfield, Labavitch, & Bennett, 1998; Rosli, Civello, & Martinez, 2004; Santiago-Doménech et al., 2008), a moderate loss of galactose and arabinose (Redgwell, Fischer, Kendal, & MacRae, 1997b), as well as a reduction in the hemicellulosic content (Huber, 1984; Lee & Kim, 2011; Rosli et al., 2004). In general, ionic and covalently bound pectins, those extracted with chelating or alkaline reagents, respectively, are the cell wall pectin fractions that suffer the most dramatic changes during fruit softening (Brummell, 2006; Mercado, Pliego-Alfaro, & Quesada, 2011). In strawberry, these pectins fractions have been identified as a key component of fruit texture, since the down-regulation of a pectate lyase (Jiménez-Bermúdez et al., 2002; Santiago-Doménech et al., 2008) or a polygalacturonase gene (Quesada et al., 2009) reduced both fruit softening and the above mentioned ripening-related changes in cell wall pectins. However, the quantitative and qualitative biochemical changes observed were not easily related to the change in texture which is physical in nature. A more detailed analysis of the pectic polysaccharides molecules present in these fractions is required to achieve a better understanding of the inter-relationship between pectin structure and fruit texture during strawberry softening. In this context, the atomic force microscope (AFM), first described by Binnig, Gerber, Stoll, Albrecht, and Quate (1987), is a powerful technique that allows characterization of complex and heterogeneous samples at the molecular level. AFM has successfully provided three-dimensional images of the surface topography of biological molecules such as DNA (Strick, Allemand, Bensimon, Bensimon, & Croquette, 1996), proteins (Gunning et al., 1996), and polysaccharides (Kirby, Gunning, Waldron, Morris, & Ng, 1996b; Morris, Gromer, Kirby, Bongaerts, & Gunning, 2011; Morris et al., 1997; Ovodov, 2009; Round, Rigby, MacDougall, & Morris, 2010), including pectins (Kirby, Gunning, Morris, & Ridout, 1995). AFM can be used to study materials with just minor sample preparation and provides a valuable tool for studying polysaccharide conformation in conditions that more closely mimic their natural environment. AFM imaging allows information to be obtained on the contour length distribution and the branching of polysaccharides complementing values obtained by size exclusion chromatography (SEC). SEC provides physical characterization of molecules based on the average properties of a whole group of pectin molecules with similar hydrodynamic properties, whereas the AFM imaging gives information on individual isolated pectin molecules. Thus at present it is useful to supplement conventional SEC and FTIR analysis with new molecular values from AFM to elucidate a clearer picture of pectin structure.

The main goal of the present study was to use AFM conditions to visualize and characterize different ionic and covalently bound pectic fractions from strawberry cell wall samples. This has shed new light on the molecular heterogeneity and branching of strawberry pectin polymer extracts. The AFM results were complemented with measurements of sugar composition, ATR–FTIR and SEC analysis.

2. Materials and methods

2.1. Polysaccharide extraction

The method used for the isolation of the cell wall material (CWM) from ripe strawberry fruits (*Fragaria* × *ananassa*, Duch., cv. Chandler) was based on the protocol of Redgwell, Melton, and Brasch (1992) with modifications, as described previously by Santiago-Doménech et al. (2008). The cell wall preparations were sequentially extracted as described previously (Santiago-Doménech et al., 2008) to obtain CDTA (ionically bound) and Na_2CO_3 (covalently bound) soluble fractions for further analysis. Extensive dialysis was used to obtain pectin fractions of high purity free from salts and fractionation reagents. Both the CDTA and carbonate pectin fractions were stored until required as aqueous solutions at −20 °C, in order to avoid possible aggregation induced during freeze-drying. Aliquots of 1 ml were lyophilised for FTIR and SEC analysis. Extraction and fractionation process were performed in triplicate.

Neutral sugar content was determined by the orcinol method (Rimington, 1931; Tillmans & Philippi, 1929) using glucose as standard. UA was determined by the carbazole method (Filisetti-Cozzi & Carpita, 1991) with slight modifications using GalA as standard. Absorbance data were corrected as described by Montreuil, Spik, Fournet, and Tollier (1997) in order to eliminate interferences from neutral sugars, and UA, in the carbazole and orcinol methods, respectively.

2.2. Fourier transform infrared spectroscopy

Infrared spectra were obtained with an Attenuated Total Reflectance (ATR) accessory (MIRacle ATR, PIKE Technologies, USA) coupled to a Fourier transform infrared (FTIR) spectrometer (FT/IR-4100, JASCO, Spain) as described previously (Heredia-Guerrero, San-Miguel, Sansom, Heredia, & Benítez, 2010). Briefly, the freeze-dried samples were mounted on top of the ATR crystal and compressed gently with a sample clamp whilst monitoring the spectral absorbance. All spectra were recorded in the 4000–600 cm^{-1} range with a resolution of 4 cm^{-1} and averaged over 25 scans. ATR effect and atmospheric contributions from carbon dioxide and water vapour were corrected by means of the Spectra Manager v.2 software (JASCO, Spain) over the full spectral range.

2.3. Size exclusion chromatography

A manually poured column (c10/40, GE healthcare) of Sepharose CL-2B (Sigma–Aldrich Química SA, Spain) was used to fractionate the polymers present in the CDTA and Na_2CO_3 fractions within the molecular mass range 100–20 × 10^3 kDa (for dextrans/pullulans). Gel media were equilibrated with 0.2 M acetate buffer, pH 5, for CDTA samples and Tris–HCl 0.05 M, pH 8.5, for Na_2CO_3 samples. Cell wall fractions (3–5 mg) were dissolved in 1 ml of the same buffers used for gel equilibration. The loading volume was 250 μl and the elution flow rate was 10 ml h^{-1}. Fractions (1 ml) were collected and assayed for UA and neutral sugar contents as previously

described. The void (V_0) and the total (V_T) volumes of the columns were obtained by using dextran blue and acetone, respectively.

2.4. Atomic force microscopy

CDTA samples were processed as described for tomato cell wall fractions (Kirby, MacDougall, & Morris, 2008; Round, Rigby, MacDougall, Ring, & Morris, 2001). The samples were sonicated for 10 min to facilitate dissolution. For the Na_2CO_3 pectin samples the procedure was slightly different; the samples were heated to 80 °C for 10 min to aid dissolution and then diluted in distilled water without sonication. The stock solutions were diluted with 10 mM ammonium bicarbonate buffer, pH 8, to a final concentration of 1–5 μg ml^{-1}. Three microlitres samples were then drop-deposited onto freshly cleaved sheets of mica (G250, Agar Scientific). The coated mica preparations were air-dried on a heating block at 37 °C, in order to promote even spreading of the sample across the mica, to reduce molecular aggregation on drying, and to sublime off the buffer (Kirby et al., 2008). Once the sample had dried (20 min) it was inserted into the liquid cell of the microscope. Triple distilled butanol (300 μl) was injected into the cell halfway through the sample approach sequence. The use of butanol as an imaging solvent has a double purpose: it eliminates capillary condensation effects and, as a precipitant, it limits desorption during imaging (Kirby, Gunning, & Morris, 1996a; Round et al., 2001).

The AFM used for the present studies was manufactured by ECS (East Coast Scientific Limited, Cambridge, UK). Short tip variety AFM probe model contact cantilevers (Budget Sensors, Bulgaria) were used with a quoted resonance frequency and force constant of 13 kHz and 0.4 N m^{-1}, respectively. A low-power light microscope, equipped with a television camera, was used to roughly position the AFM probe onto the top of the sample. The imaging was operated in contact mode with a scan speed of 2 Hz. Both, topographical and error-signal mode images were collected simultaneously.

The heights of features in the images were analyzed using the AFM software supplied with the instrument (SPM 6.01, ECS, Cambridge, UK). For the length measurements, images were converted to TIFF files using Paint Shop Pro v5.00 software. Image contrast was optimised using Adobe Photoshop CS2 software. Then, AFM images were analyzed off-line using Image J v1.43u software. The length of single pectin chains was determined by plotting the main chain with the freehand tool of the software. To determine the chain lengths, individual molecules were defined as strands that were not entangled with, or overlapping other strands, that were long enough to be exactly visualized, and which lay entirely within the scanned area (Adams, Kroon, Williamson, & Morris, 2003). Furthermore, other features were also characterized, including the number of branch points and branch lengths. Height measurements were used to judge whether the chain contained a true branch point: at genuine branch points the height remain unchanged whereas if two chains lie on top of each other the height will double (Round et al., 2001).

2.5. AFM image analysis

The pectin samples studied contain individual polymers which can be characterized by their length distributions. In this work, we have used two representations. The experimental data has been plotted as histograms where the frequency of occurrence of particular lengths has been plotted against the molecular length. The histograms were found to be well approximated by the Log normal skew distribution and these fits were used to generate cumulative frequency curves.

The Log normal distribution f(L) of particle lengths (L) is of the form:

$$f(L) = [\sigma_s L(2\pi)^{1/2}]^{-1} \exp\left[-0.5\left\{\sigma_s^{-1}\left(\ln\left(\frac{L}{m}\right)\right)\right\}^2\right]$$

where the parameter m (geometric mean) has the dimensions of length and the parameter σ_s defines the deviation about the mean. These parameters describe the position and shape of the distribution with respect to the particle length (L). The distribution function is normalized by $\int f(L) = 1$ when integrated over the range $L = 0$–∞. The moments of the distribution function yield different average lengths for the distribution. In this study, we have calculated the number-average (L_N) and the weight-average (L_W) contour lengths and their ratio (L_W/L_N) or polydispersity index (PDI) (Odian, 2004). In this case for a Log normal distribution $L_N = m\exp(\sigma_s^2/2)$, $L_W = m\exp(3\sigma_s^2/2)$ and $L_W/L_N = \exp(\sigma_s^2)$. More than 350 individual measurements from independent images were employed to obtain the length distribution representations and statistical parameters.

2.6. Statistical analysis

The SPSS software package (v.19.0, IBM Corp., Route 100, Somers, NY) was used for all the statistical analysis. For the AFM study, one hundred images per sample were collected to obtain representative data of the pectin samples. A minimum of 350 independent measurements, obtained from different images, were used for statistical comparisons with the SPSS software. The original data distributions were compared with Kruskal–Wallis test. The parameter ME is the median of the original data. Original data were also transformed by natural logarithm to obtain normal distributions which were compared by analysis of variance (ANOVA). The distribution of ln(L) is a normal distribution: the symmetrical nature of this distribution, in which the peak value and the upper and lower bounds of ln(L) are well-defined, mean that the median of ln(L) and its standard deviation can be used to determine better estimates of the parameters m and σ_s for the skew distribution.

Differences in the branching of the polymer chains, presence/absence of side chains and the number of side chains per backbone, were analyzed by Chi-square test at $P = 0.05$.

3. Results

3.1. Sugar composition analysis

Cell wall material (CWM) was extracted from ripe strawberry fruits and sequentially treated with CDTA and Na_2CO_3 to obtain the ionic and covalently bound pectin fractions, respectively. The average cell wall content per 100 g of fruit frozen tissue obtained was 0.68 ± 0.02 g. As expected for pectic fractions, both types of extract showed a high content of UA, with 88 and 67% UA in CDTA and carbonate fractions, respectively. The CDTA-extracted fraction is enriched in pectin molecules associated with the middle lamellae (Redgwell & Selvendran, 1986; Selvendran, 1985) and its neutral sugar content was significantly lower than that in the sodium carbonate fraction. Na_2CO_3 is believed to extract pectins covalently linked within the primary cell wall (Redgwell & Selvendran, 1986; Selvendran, 1985) this fraction contained 35.4 ± 3.06 mg Glc g^{-1} CWM, almost four times higher than the CDTA extracts, with 9.03 ± 1.24 mg Glc g^{-1} CWM.

3.2. ATR–FTIR analysis

Fig. 1 shows the FTIR region 1900–800 cm^{-1} of the CDTA and carbonate pectin extracts. The profile of the CDTA fraction showed

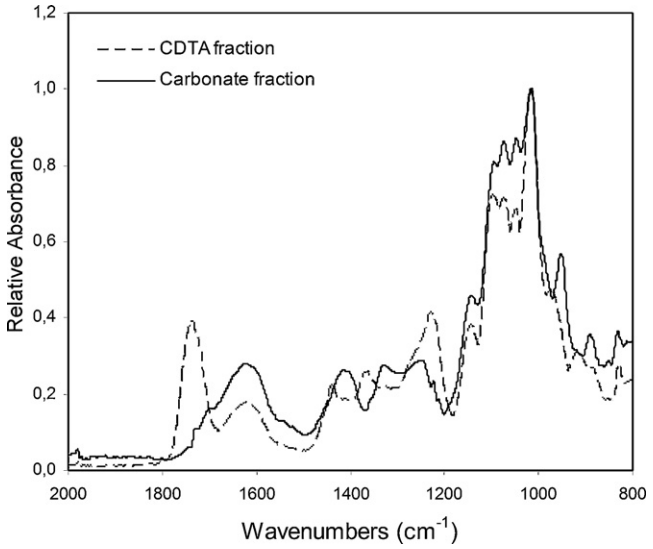

Fig. 1. ATR–FTIR absorbance spectra of CDTA (dashed line) and Na_2CO_3 (filled line) pectic fractions in the 2000–800 cm^{-1} region.

a peak at ~1737 cm^{-1}, characteristic of esterified pectins, arising from the ester carbonyl stretching band. In the carbonate fraction this peak disappeared as a result of the elimination of ester linkages during the alkaline extraction. Consequently, in this fraction, the absorption at ~1625 and ~1415 cm^{-1} increased due to the antisymmetric and symmetric COO^- stretching bands. Interestingly, the ester band in the CDTA fraction showed a shoulder at 1720 cm^{-1} which is diagnostic for phenolic esters (Sene, McCann, Wilson, & Grinter, 1994). Moreover, the CO stretching vibration band at approximately 1240 cm^{-1} was higher in the CDTA extract than in Na_2CO_3 sample, showing the former had a higher UA content. The fingerprint region, 1200–900 cm^{-1}, can be used to identify particular polysaccharides in the samples. In the CDTA fraction, this region showed the strongest peaks at 1016 and 1100 cm^{-1}. Carbonate pectin profiles also showed their strongest peak at 1016 cm^{-1}. However, the band at 1100 cm^{-1} diminished whereas the absorbance at 1075, 1047 and 953 cm^{-1} increased in Na_2CO_3 extract, suggesting a different sugar composition. The absence of amide bands (amide I: 1670 cm^{-1}; amide II: 1588 cm^{-1}) in both polymer fractions indicated that they are mainly composed of pectin and apparently free of detectable protein.

3.3. Size exclusion chromatography profiles

The uronide and neutral sugar profiles obtained for both pectin fractions are shown in Fig. 2. Polyuronides present in the CDTA fraction eluted throughout the entire fractionation range of the column, showing three peaks with similar concentration (Fig. 2A). The neutral sugar polymer profile for this fraction was low although three small residual peaks were observed (Fig. 2B). This is in accordance with the ~90% of uronic acid content of this fraction.

As expected, the concentration values for the polyuronide profile of the Na_2CO_3 fraction were lower than those shown for the CDTA extract (Fig. 2A). A small first peak eluted close to 15 ml but the main peak of this fraction has a lower molecular mass and it eluted at 27.5 ml. This indicates that this fraction has a relatively higher amount of low molecular mass polymers. It is noteworthy that a sharp peak at the same elution volume is resolved in the neutral sugar profile (Fig. 2B). This reflected the higher amount of neutral sugar present in this fraction when compared with the CDTA fraction (Section 3.1). Summarizing, the SEC analysis showed that the main differences between CDTA and Na_2CO_3 polymers

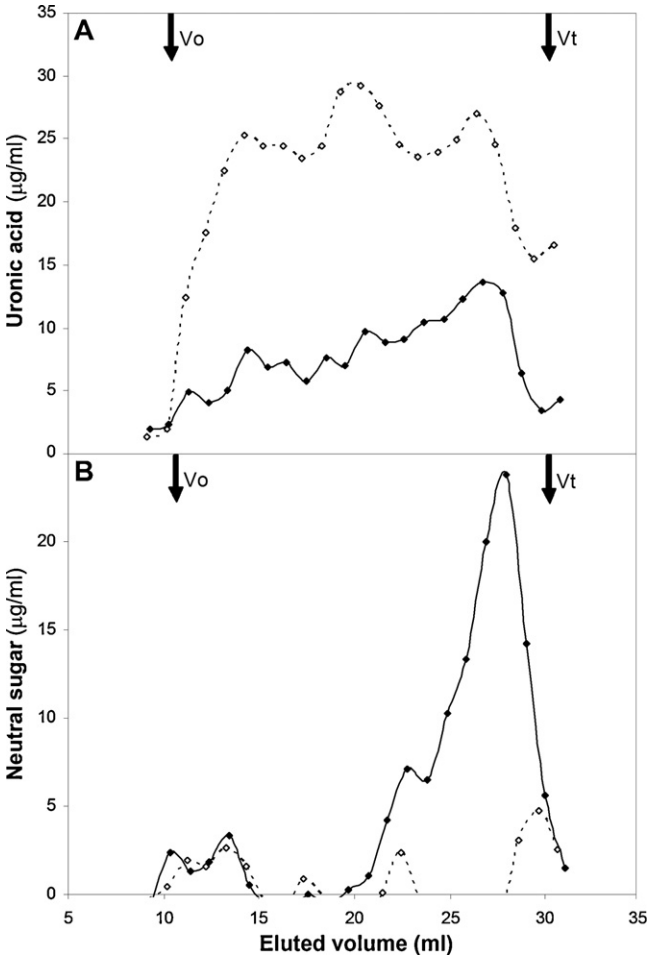

Fig. 2. Comparative SEC molecular profiles of polysaccharides extractable by CDTA (dashed lines) and Na_2CO_3 (filled lines) solutions from cell walls of ripe strawberry fruits obtained by SEC on Sepharose CL-2B columns. Fractions were assayed for uronic acid (A) and neutral sugar (B) content. Void volume (V_0) and total volume (V_T) are indicated on the figures.

were a higher content of uronic acids in the CDTA fraction, a higher representation of neutral sugars in the Na_2CO_3 extract, and a lower molecular mass for both acid and neutral sugar containing polymers in the later fraction.

3.4. AFM analysis

Fig. 3 shows representative AFM images of the CDTA and Na_2CO_3 samples. In both cases, linear filamentous structures were present with a small proportion of them possessing branches. Furthermore, some aggregates, distinguishable by height measurements were also present, even at low sample dilutions when very few individual polymers were present in the samples. This observation suggests that they are not simply superpositions or entanglements of polymers caused by the reduction of solvent volume during drying down on to the substrate, but are multi-polymer complexes held together by intermolecular interactions. The consistent presence of these polymers and aggregates reflects the heterogeneity and complexity of the pectin polysaccharides present in both cell wall fractions. The presence of a mixture of individual polymers and micelle-like structures in the present extracts is consistent with similar observations on pectin extracts from unripe tomato and sugar beet cell walls (Kirby et al., 2008; Round, MacDougall, Ring, & Morris, 1997; Round et al., 2010, 2001). In agreement with the broad profiles observed by SEC the contour lengths of the linear and

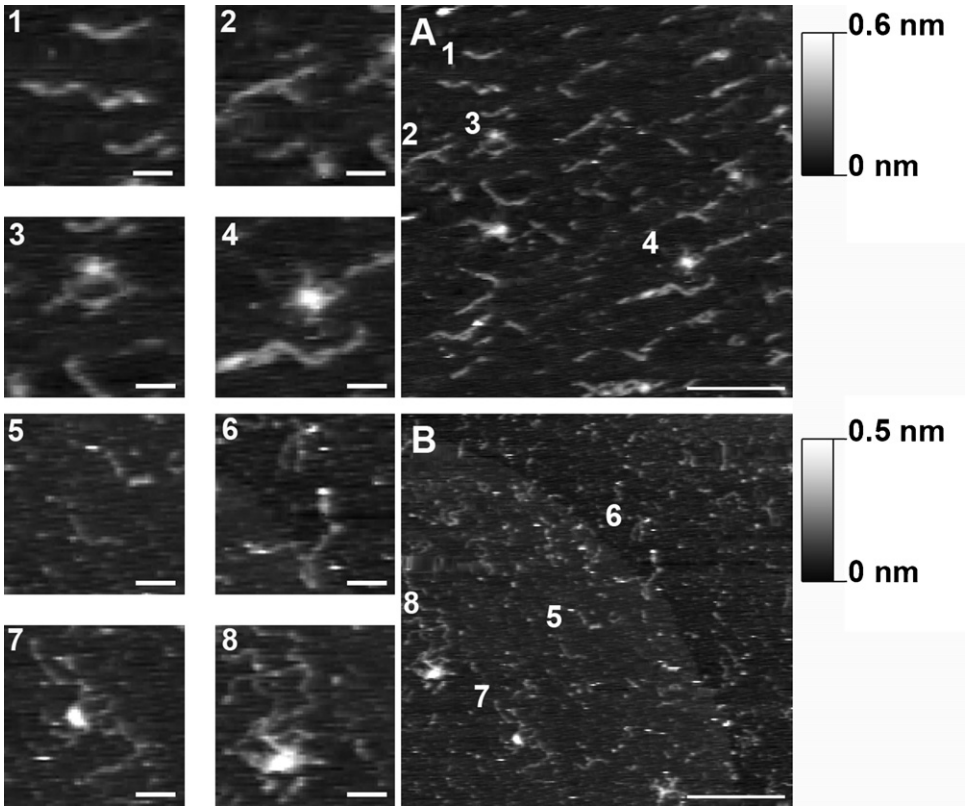

Fig. 3. Representative topographical AFM images of CDTA (A) and Na_2CO_3 (B) pectin extracts after drop deposition onto mica. Inserts (1–8) show zoomed areas from the A and B images to show examples of single linear chains (1 and 5), branched chains (2 and 6) and aggregates or multi-polymer complexes (3, 4, 7 and 8), respectively. AFM images are accompanied by height scale bars showing the dz value (highest height during the scan). The scale bars for A–B are 250 nm, whilst the scale bars for the inserts 1–8 are 50 nm.

branched individual polymers ranged in size from tens to hundreds of nanometres. Also in the sodium carbonate fraction individual polymers were shorter and the shape of the aggregates was seen to be slightly different to those seen in the CDTA fraction. Initially, the CDTA and Na_2CO_3 samples were processed with the same protocol but, in these early experiments, conspicuous thick aggregates were visualized in the Na_2CO_3 samples (Fig. 4). These types of structures have not been reported previously for sodium carbonate pectin extracts, but the fibrous and aggregated polymers present in the background were similar to those observed in extracts from tomato and sugar beet (Kirby et al., 2008; Round et al., 2001). At first it was thought these structures might be non-pectin components of the cell wall. The thick aggregates were pelleted using 10 min centrifugation at 12,000 × *g* and the pellet was analyzed by ATR–FTIR. The spectrum obtained showed the typical pectin fingerprint in the 1200–900 cm^{-1} region (data not shown). The presence of these big

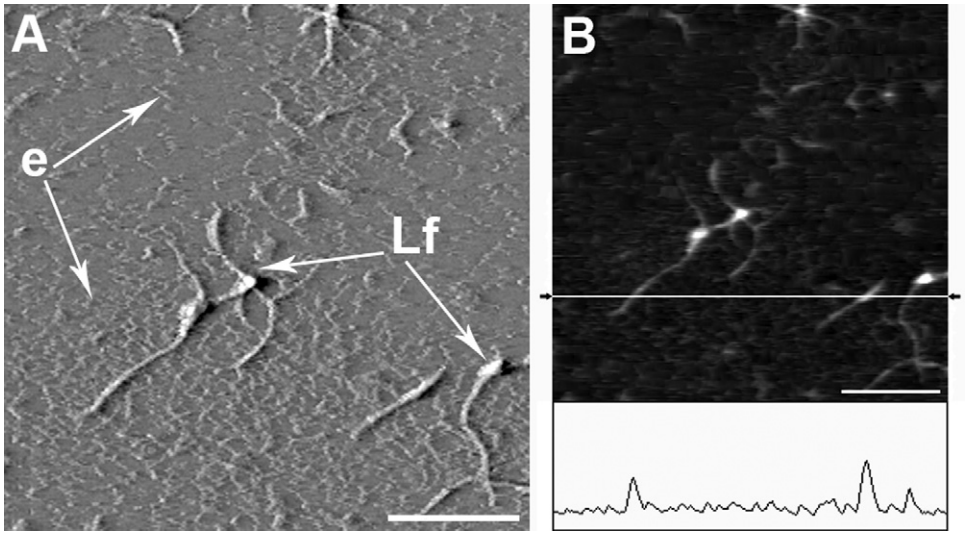

Fig. 4. (A) AFM error signal mode image of Na_2CO_3 samples drop deposited onto mica showing the large fibrous aggregates (Lf) and the expected mixture of elongated pectins and micellar aggregates (e) in the background. (B) Topographical mode image with height profile, from same scan as A. The line profile illustrates the differences in height between the big fibres (2, 1.4 and 1 nm) and the individual molecules in the background (0.4 ± 0.1 nm). Maximum height value or dz: 2 nm. The scale bars for A–B are 250 nm.

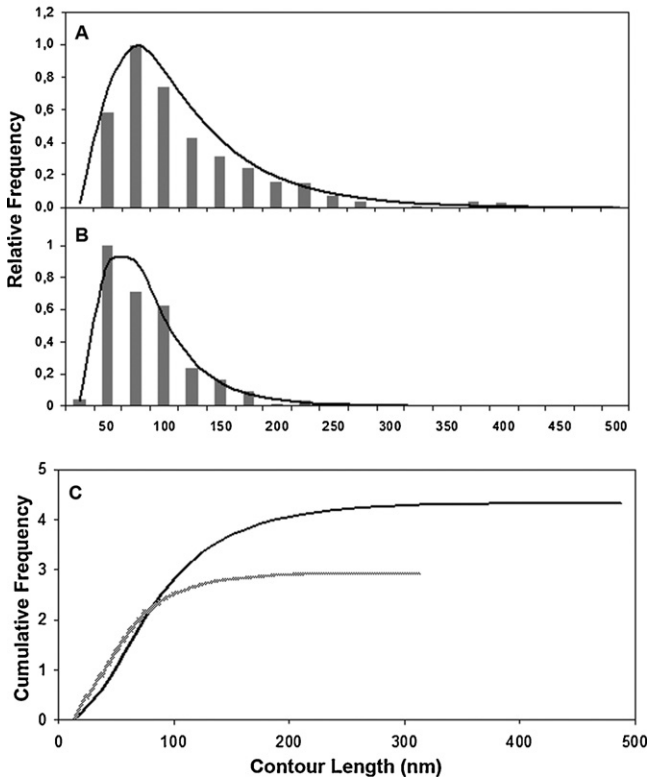

Fig. 5. Contour length distribution from CDTA (A) and sodium carbonate (B) soluble polymers. Bars represent observed data whilst the curved lines represent Log normal approximations. (C) Cumulative frequencies for CDTA (black line) and Na_2CO_3 (grey line) pectic fractions by Log normal function normalized to the maximum peak obtained in each profile. $N = 379$ and 372 for CDTA and Na_2CO_3 samples, respectively.

fibres dominated the grey levels in the image making it difficult to obtain good resolution images of the individual molecules and micellar aggregates in the background. Several treatments were tried to disperse the big fibres. Finally, it was found that dilution with distilled water, instead of ammonium bicarbonate buffer, and heating the solutions at 80 °C (see Section 2.4) solubilised these thick aggregates as shown in Fig. 3B.

The individual molecules were characterized in terms of histograms of their contour length distributions for both fractions (Fig. 5). The length distribution for CDTA pectin fraction was in the range of 20–500 nm whilst Na_2CO_3 fraction distribution ranged between 20 and 320 nm. Both set of data were right-skewed and well approximated by a Log normal distribution, as represented in Fig. 5. The polymers extracted with CDTA were generally longer and distributed over a wider range of lengths than those extracted with sodium carbonate. Both distributions can be easily compared when the results are plotted as cumulative frequencies (Fig. 5C). Table 1 shows the number-average (L_N) and the weight-average (L_W) contour lengths and the polydispersity indexes (PDI) of the polymers present in both fractions. These three parameters were higher in the CDTA samples. Additionally, statistic parameters are also shown in this table. The statistical comparison of both distributions by the Kruskal–Wallis test showed that they were significantly different at $P = 0.05$. The medians (ME) were statistically different by non parametric test ($P = 0.05$). As expected, ME values are very similar to theirs geometric means (m) of the CDTA and Na_2CO_3 fractions, respectively (Table 1), because both are different estimates of the position parameter of the Log normal distributions. The original data were log-transformed and the normal distribution compared and found to be different by the ANOVA test: their transformed means also being statistically different. The shape parameter (σ_s) was slightly higher in the CDTA samples, and this wider range can be also observed when cumulative frequencies are represented (Fig. 5C).

Table 1
Descriptors of contour length distributions of CDTA and Na_2CO_3 pectins extracted from ripe strawberry fruits obtained from AFM images. ME corresponds to the median value of (L). Values followed by different letters within the same row are significantly different at $P = 0.05$ (non-parametric median test for original data and ANOVA test for normalized data). $N = 379$ and $N = 372$ for CDTA and Na_2CO_3 samples, respectively. The parameters μ^* (mean) and σ^* (standard deviation) characterize the nomal distribution of ln(L).

	CDTA	Na_2CO_3
L_N (nm)	108	74
L_W (nm)	157	98
PDI	1.46	1.32
ME (nm)	86a	65b
Log normal distribution		
m (nm)	89.1	64.47
σ_s	0.61	0.53
Normalized distribution		
μ^* (nm)	4.49a	4.17b
σ^*	0.55	0.52

Table 2
Branching characteristics of the CDTA and Na_2CO_3 pectin extracts from ripe strawberry fruits as obtained from the AFM images. Values followed by different letters within the same file are significantly different by Chi-square test at $P = 0.05$. $N = 33$ and $N = 39$ for CDTA and Na_2CO_3 samples, respectively.

	CDTA	Na_2CO_3
Lb_N (nm)	65	29
Lb_W (nm)	89	37
PDI	1.37	1.29
Branching (%)	8.4a	9.4a
Multibranching (%)	3	9

For both CDTA and Na_2CO_3 pectin fractions the level of branching was about 9%, but the percentage of multi-branched polymers was higher in Na_2CO_3 (~9%) than in CDTA (~3%) samples (Table 2). Several examples of typical branched pectin molecules are shown in zoomed areas (2 and 6) of Fig. 3. The lengths of the branches (Lb) present in the CDTA polymers yields average values of Lb_N of 65 nm and Lb_W of 89 nm with a PDI value of 1.37. Average lengths of the branches in the Na_2CO_3 samples were 29 and 37 nm for Lb_N and Lb_W, respectively, with a PDI value of 1.29. Thus, CDTA branches were approximately 60% longer than Na_2CO_3 branches. Furthermore, the ratio of the backbone length to branch length was 1.8 for both fractions. The branch length data could not be fitted to a Log normal distribution, probably because a higher number of branch measurements are needed to get the sufficient data for a more detailed and significant distribution analysis.

4. Discussion

4.1. Composition and general physicochemical characterization of the cell wall fractions

CDTA and sodium carbonate are typically used to enrich extracts for pectins that are ionically or covalently bound to the cell wall matrix, respectively (Lara, García, & Vendrell, 2004; Redgwell et al., 1992; Santiago-Doménech et al., 2008; Selvendran, 1985). In both fractions, the total UA and neutral sugar contents were in the same range of values reported by several authors for ripe strawberry fruit cell walls (Jiménez-Bermúdez et al., 2002; Koh & Melton, 2002; Quesada et al., 2009; Redgwell et al., 1997a; Santiago-Doménech et al., 2008). As expected, both fractions showed a high content of UA which reached ~88% of the total sugar content in the CDTA fraction and ~67% in the Na_2CO_3 fraction.

The CDTA fraction is believed to be enriched in partially esterified homogalacturonan pectin components from the middle lamella (Lara et al., 2004; Redgwell et al., 1992) and the neutral sugar content is low. FTIR spectra of this fraction confirmed this suggestion. Carbohydrates show a strong absorbance in the region 1200–900 cm^{-1}, due to ring vibrations overlapped with stretching vibration of the hydroxyl groups and the glycosidic bond vibration (Filippov, 1992; Kacuráková, Capek, Sasinková, Wellner, & Ebringerová, 2000). Both strawberry pectin fractions showed spectral profiles in this region similar to those reported for polygalacturonic acid (Wellner, Kacuráková, Malovíková, Wilson, & Belton, 1998), with four bands at about 1016, 1047, 1075 and 1100 cm^{-1}. However, the bands at 1016 and 1100 cm^{-1} of the CDTA FTIR spectra were stronger than those obtained with the Na_2CO_3 samples, as described by Kacuráková et al. (2000) for pectin with high homogalacturonan content and by Coimbra, Barros, Barros, Rutledge, and Delgadillo (1998) for pectin samples rich in uronic acid. FTIR spectra of the CDTA fraction also demonstrate that the exhaustive dialysis employed in the present study effectively eliminated CDTA contamination since spectra of CDTA-solubilised pectin did not overlap with the peaks of the CDTA salt, with maximum absorbance bands at 1704, 1579 and 1216 cm^{-1}. The polyuronide SEC profile of this fraction showed the presence of three peaks, as previously reported by Santiago-Doménech et al. (2008), with slight quantitative differences. Redgwell et al. (1997a) also reported CDTA polymers elution throughout much of the fractionation range for CL-2B sepharose column with a different strawberry cultivar.

Na_2CO_3 is considered to solubilise pectic polymers by breaking ester linkages to mainly release pectin from the primary cell wall. The quantitative results agree with this assumption and the Na_2CO_3-extracted fraction was found to be richer in neutral sugars than the CDTA fraction. Furthermore, the UA and neutral sugar contents of this fraction were similar to homologue fractions obtained in previous studies (Fraeye et al., 2009; Rosli et al., 2004). As expected, the ester peak at about 1740 cm^{-1} was absent in the FTIR spectra of the Na_2CO_3-soluble fraction indicating that de-esterification occurred as result of the extraction procedure. Similar results have been obtained by Osorio et al. (2008) with pectins extracted from *Fragaria vesca* fruits. Interestingly, the absorbance bands at 1075 and 1047 cm^{-1} of the fingerprint region increased, and this could indicate that this fraction is enriched with the rhamnogalacturonan I pectic domain. Kacuráková et al. (2000) reported that RGI showed maximum absorbance at about these wave numbers, and assigned the 1075 and 953 cm^{-1} peaks to the galactose units and 1047 cm^{-1} peak to arabinose units (Coimbra et al., 1998). This higher content of neutral sugar is also confirmed by the sugar SEC profile of this fraction (Fig. 2B).

Finally, as mentioned in Section 3.2, the absence of bands at 1670 and 1588 cm^{-1} indicates that the protein content in both pectin fractions was low or negligible.

4.2. Nanostructural analysis by AFM of the cell wall fractions

AFM is a powerful technique for characterizing the nanostructural conformation of macromolecules as shown in previous works on polysaccharides from fruit cell walls (Fishman & Cooke, 2009; Kirby et al., 2008; Round et al., 2001; Yang, Chen, An, & Lai, 2009). The AFM images reveal the presence of individual fibrous molecules and aggregates. For the individual polymers contour lengths distribution, level of branching and branch lengths can be obtained from the AFM images to reconstruct a conceptual picture of the polysaccharide's structure and expand our knowledge.

When this experimental work was performed instead of completed there were no previous reports on the cell wall analysis of pectin extracts by AFM for strawberry fruit. Thus, the methodology employed for sample processing and image analysis was initially based on previous and reliable protocols used in tomato cell wall studies (Kirby et al., 2008; Round et al., 2010, 2001). These methods worked for the CDTA strawberry cell wall fraction and good images for analysis were obtained. However, in the case of Na_2CO_3 samples the presence of large fibrous aggregates made it difficult to image and analyze the individual molecules in these cell wall fractions. As far as we know the presence of these structures (Fig. 4) has not been previously reported and their ATR–FTIR profile showed that they are pectins, and discarded the possibility of contaminated or protein-mediated interactions. The fibrous aggregates were not observed in the CDTA extracts. These aggregates were not covalently linked because they could be dissolved in distilled water after heating to 80 °C for 10 min. The possibility of the existence of residual calcium bridges in this fraction was also discarded because when the Na_2CO_3 fraction was treated with imidazole these large aggregates did not disappear (results not shown). The treatment used to avoid their presence was mild and completely different from those used to break covalent borate bridges from RGII (Ishii et al., 1999). Whether or not these structures are an artefact of the extraction procedure, or whether they may have some *in muro* role in the cell wall needs further research.

As seen in previous studies for cell wall of tomato and sugar beet (Kirby et al., 2008; Round et al., 2010, 2001), the strawberry CDTA and Na_2CO_3 pectin fractions contained a mixture of aggregates and both linear and branched molecules (Fig. 3). A reliable comparison of the population of the polymers present in both fractions required a high number of independent measurements obtained from different images. In our case a minimum of 350 values per fraction were needed to obtain the length distribution profiles shown in Fig. 5. In the literature, it has been accepted a minimum of 50 values to provide robust results but most studies include several hundreds (Adams et al., 2003; Abu-Lail & Camesano, 2003; Balnois et al., 2000; Round et al., 2001). As shown in Fig. 5, length data of both fractions fitted quite well to Log normal distributions which are not unusual in biological sciences (Limpert, Stahel, & Abbt, 2001). The differences found in the original distribution were maintained when the distributions were normalized and parametric statistic methods employed for comparison. On the other hand, complex pectin samples are usually characterized by their number-average molecular weight (M_N) and their weight-average molecular weight (M_W). These parameters are usually determined from viscometry and/or light scattering assays of the samples and such data is not available in this study. The SEC data can be converted into molecular mass data through the use of molecular weight standards such as pullulan molecules. The latter are flexible coil-like molecules and their use as standards would significantly overestimate the molecular masses of the pectin fractions because of the extended fibrous nature of the molecules as seen by AFM. Similarly light scattering studies would also overestimate the molecular mass because of the presence of the aggregates in the sample. The AFM results were described by directly measured length units (nm) instead of mass units (kDa), and the distribution has been used to calculate the number-average (L_N) and weight-average (L_W) contour lengths. These values can be converted to masses if the mass per unit length of the pectin structure is known. The extended fibrous nature of the observed pectin molecules suggests they can be approximated by a helical structure. The lengths were higher in the CDTA samples than in the sodium carbonate fractions. L_N and L_W values for strawberry CDTA fractions were 108 and 157 nm, respectively. Based on a 3_1 helix (Walkinshaw & Arnott, 1981) with a pitch of 1.34 nm, the equivalent molecular weights are M_N = 38,759 and M_W = 56,344. The molecular lengths are similar to those reported for CDTA fractions extracted from mature green tomato (132 and 174 nm) and from sugar beet (108 and 137 nm) (Kirby et al., 2008). A recent report on the effect of calcium treatment on strawberry cell walls did not include length measurements for single chains in this

fraction (Chen et al., 2011). Concerning the Na_2CO_3 fraction, L_N and L_W values were 74 and 98 nm, with molecule lengths ranging from 20 to 320 nm. Once again, based on a 3_1 helix (Walkinshaw & Arnott, 1981) with a pitch of 1.34 nm, the equivalent molecular weights are M_N = 26,557 and M_W = 35,170. In the case of tomato, molecule lengths of the Na_2CO_3 extracts obtained from mature green fruits ranged from 20 to 400 nm (Round et al., 2010) and no values for L_N and L_W were reported. In the previously mentioned report by Chen et al. (2011) they indicated an average length of 671 nm for pectin extracted with a mixture of Na_2CO_3 and CDTA (50 mM/2 mM). This last work compared the effect of calcium treatments on pectic chain length and branching but the number of single measurements per treatment was too low, 11–24 data values depending on the treatment, to allow a good representation and comparison of the chain population distribution. Interestingly, in peach cultivars of contrasting firmness, the same authors reported average chain length much shorter for this fraction using a higher number of measurements: 249 ± 256 nm (N = 138) for a crispy cultivar and 57 ± 27 nm (N = 40) for a soft cultivar (Yang et al., 2009). In this last cultivar, chain length ranged from 20 to 100 nm, results much more similar to our values for strawberry, which is a soft fruit. Furthermore, the size exclusion chromatography profiles of our CDTA and Na_2CO_3 fractions showed that the carbonate extracts were enriched in pectic polymers of lower molecular mass (higher elution volumes) (Fig. 2). Although this type of analysis is based on a bulk property of the pectin polymers present in the fraction, a narrower range of chain lengths and the lower values for L_N, L_W, and length median of chain present in the Na_2CO_3 fraction would correlate with such a chromatographic profile. Similar chromatographic results have been reported for other fruits. SEC profiles of CDTA and Na_2CO_3 fractions from ripe avocado and tomato also showed the presence of a peak of high molecular mass in the CDTA fraction that was absent in the carbonate fraction (Brummell & Labavitch, 1997; Huber & O'Donoghue, 1993).

The acid hydrolysis of the pectin extracts from tomato (Round et al., 1997, 2010, 2001) suggests that the branching observed by AFM is branching of the homogalacturonan backbone. The low level of branching observed means that this would be difficult to detect by classical chemical and physical methods, but it can be visualized by AFM (Kirby et al., 1996a). Both pectin fractions showed a similar percentage of branched structures (8–9%), lower than the 30% reported for similar fractions extracted from mature green tomato and the 17% observed for sugar beet pectin (Kirby et al., 2008; Round et al., 2001). In strawberry, Chen et al. (2011) mentioned the presence of fewer branches in the sodium carbonate-soluble extract based on qualitative observations. Taking into account all these results, the putative RG-I enrichment of the Na_2CO_3 fraction with its side chains of arabinose and galactose (hairy regions) does not results in a higher branching percentage for this fraction, in spite of its higher neutral sugar content. In fact, recent evidences based on AFM studies of pectin samples subjected to mild acid hydrolysis support that neutral sugars are present as short branches, not detected by AFM, whereas longer branches detected by AFM are composed of polygalacturonic acid, as previously proposed by Round et al. (2010). Despite the similar percentage of branching, the images showed a different pattern of branching for both fractions. Whilst the CDTA polymers showed longer branches, the Na_2CO_3 polymers showed smaller but more branches per backbone. Differences in branching patterns have also been described in amylose samples (Gunning et al., 2003). The existence of long branches and aggregates complicates the conventional interpretation of viscosity and light scattering data in terms of deriving simple relationships between the chemical composition and the measured average molecular weight, without taking into account the contribution of the branched or aggregated components.

In summary, the present work complements previous characterization of strawberry cell wall fractions with reliable data at the nanostructural level. Pectins extracted with chelating agents, supposedly located in the middle lamella, contained a higher proportion of uronic acids and were significantly longer than those covalently bound within the primary cell wall. The level of branching was, however, similar in both pectin fractions (ca. 9%), although a higher proportion of multi-branching polymers were detected in carbonate pectin extracts. Branch lengths were also higher in CDTA pectins. The micellar aggregates are more difficult to characterize. However, the level of these aggregates was similar for both the CDTA and Na_2CO_3 fractions. The ratio of occurence of micellar aggregates was about 40 aggregates per 24 scans ($1\ \mu m \times 1\ \mu m$) or a rate of about 1.6 aggregates per ($1\ \mu m \times 1\ \mu m$) area of the substrate. This is equivalent to about 5–6 aggregates per 100 individual molecules.

This AFM study facilitates a better understanding of the role of the polymers present in these fractions on the cell wall disassembly process that occurs during fruit softening. Further work is being undertaken to apply this approach to selected transgenic genotypes with modified levels of pectinase enzymes.

Acknowledgements

This work was funded by the Ministerio de Educación y Ciencia of Spain and Feder EU Funds (grant reference: AGL2008-02356). S. Posé was supported with a FPI fellowship from the Spanish Government (grant reference: BES-2006-13626). The research at IFR was supported through the BBSRC core grant to the Institute. We thank Dr José M. López-Aranda for his support and advice on growing the plants and Mari C. Molina for her work in plant growth and maintenance. The authors also thank Dr Antonio Heredia Bayona for his kind support and J. Alejandro Heredia-Guerrero for technical assistance and suggestions on ATR–FTIR work. S.P. also thanks A. Patrick Gunning for technical support on AFM, and Valeria Giosafatto for hospitality in Norwich during some of the experiments.

References

Abu-Lail, N. I., & Camesano, T. A. (2003). Polysaccharide properties probed with atomic force microscopy. *Journal of Microscopy*, *212*, 217–238.

Adams, E. L., Kroon, P. A., Williamson, G., & Morris, V. J. (2003). Characterisation of heterogeneous arabinoxylans by direct imaging of individual molecules by atomic force microscopy. *Carbohydrate Research*, *338*, 771–780.

Balnois, E., Stoll, S., Wilkinson, K. J., Buffle, J., Rinaudo, M., & Milas, M. (2000). Conformations of succinoglycan as observed by atomic force microscopy. *Macromolecules*, *33*, 7440–7447.

Binnig, G., Gerber, C., Stoll, E., Albrecht, T. R., & Quate, C. F. (1987). Atomic resolution with atomic force microscope. *Surface Science*, *189–190*, 1–6.

Brummell, D. A. (2006). Cell wall disassembly in ripening fruit. *Functional Plant Biology*, *33*, 103–119.

Brummell, D. A., & Labavitch, J. M. (1997). Effect of antisense suppression of endopolygalacturonase activity on polyuronide molecular weight in ripening tomato fruit and in fruit homogenates. *Plant Physiology*, *115*, 717–725.

Chen, F., Liu, H., Yang, H., Lai, S., Cheng, X., Xin, Y., et al. (2011). Quality attributes and cell wall properties of strawberries (*Fragaria* × *annanassa* Duch.) under calcium chloride treatment. *Food Chemistry*, *126*, 450–459.

Coimbra, M. A., Barros, A., Barros, M., Rutledge, D. N., & Delgadillo, I. (1998). Multivariate analysis of uronic acid and neutral sugars in whole pectic samples by FT-IR spectroscopy. *Carbohydrate Polymers*, *37*, 241–248.

Figueroa, C. R., Rosli, H. G., Civello, P. M., Martínez, G. A., Herrera, R., & Moya-León, M. A. (2010). Changes in cell wall polysaccharides and cell wall degrading enzymes during ripening of *Fragaria chiloensis* and *Fragaria* × *ananassa* fruits. *Scientia Horticulturae*, *124*, 454–462.

Filippov, M. P. (1992). Practical infrared spectroscopy of pectic substances. *Food Hydrocolloids*, *6*, 116–142.

Filisetti-Cozzi, T. M. C. C., & Carpita, N. C. (1991). Measurement of uronic acids without interference from neutral sugars. *Analytical Biochemistry*, *197*, 157–162.

Fishman, M. L., & Cooke, P. H. (2009). The structure of high-methoxyl sugar acid gels of citrus pectin as determined by AFM. *Carbohydrate Research*, *344*, 1792–1797.

Fraeye, I., Knockaert, G., Buggenhout, S. V., Duvetter, T., Hendrickx, M., & Loey, A. V. (2009). Enzyme infusion and thermal processing of strawberries: Pectin conversions related to firmness evolution. *Food Chemistry*, *114*, 1371–1379.

Gunning, A. P., Giardina, T. P., Faulds, C. B., Juge, N., Ring, S. G., Williamson, G., et al. (2003). Surfactant-mediated solubilisation of amylose and visualisation by atomic force microscopy. *Carbohydrate Polymers*, *51*, 177–182.

Gunning, A. P., Wilde, P. J., Clark, D. C., Morris, V. J., Parker, M. L., & Gunning, P. A. (1996). Atomic force microscopy of interfacial protein films. *Journal of Colloid and Interface Science*, *183*, 600–602.

Heredia-Guerrero, J. A., San-Miguel, M. A., Sansom, M. S. P., Heredia, A., & Benítez, J. J. (2010). Aleuritic (9, 10, 16-trihydroxypalmitic) acid self-assembly on mica. *Physical Chemistry Chemical Physics*, *12*, 10423–10428.

Huber, D. J. (1984). Strawberry fruit softening: The potential roles of polyuronides and hemicelluloses. *Journal of Food Science*, *49*, 1310–1315.

Huber, D. J., & O'Donoghue, E. M. (1993). Polyuronides in avocado (*Persea americana*) and tomato (*Lycopersicon esculentum*) fruits exhibit markedly different patterns of molecular weight downshifts during ripening. *Plant Physiology*, *102*, 473–480.

Ishii, T., Matsunaga, T., Pellerin, P., O'Neill, M. A., Darvill, A., & Albersheim, P. (1999). The plant cell wall polysaccharide rhamnogalacturonan II self-assembles into a covalently cross-linked dimer. *Journal of Biological Chemistry*, *274*, 13098–13104.

Jiménez-Bermúdez, S., Redondo-Nevado, J., Muñoz-Blanco, J., Caballero, J. L., López-Aranda, J. M., Valpuesta, V., et al. (2002). Manipulation of strawberry fruit softening by antisense expression of a pectate lyase gene. *Plant Physiology*, *128*, 751–759.

Kacuráková, M., Capek, P., Sasinková, V., Wellner, N., & Ebringerová, A. (2000). FT-IR study of plant cell wall model compounds: Pectic polysaccharides and hemicelluloses. *Carbohydrate Polymers*, *43*, 195–203.

Kirby, A. R., Gunning, A. P., & Morris, V. J. (1996a). Imaging polysaccharides by atomic force microscopy. *Biopolymers*, *38*, 355–366.

Kirby, A. R., Gunning, A. P., Morris, V. J., & Ridout, M. J. (1995). Observation of the helical structure of the bacterial polysaccharide acetan by atomic force microscopy. *Biophysical Journal*, *68*, 360–363.

Kirby, A. R., Gunning, A. P., Waldron, K. W., Morris, V. J., & Ng, A. (1996b). Visualization of plant cell walls by atomic force microscopy. *Biophysical Journal*, *70*, 1138–1143.

Kirby, A. R., MacDougall, A. J., & Morris, V. J. (2008). Atomic force microscopy of tomato and sugar beet pectin molecules. *Carbohydrate Polymers*, *71*, 640–647.

Koh, T. H., & Melton, L. D. (2002). Ripening-related changes in cell wall polysaccharides of strawberry cortical and pith tissues. *Postharvest Biology and Technology*, *26*, 23–33.

Lara, I., García, P., & Vendrell, M. (2004). Modifications in cell wall composition after cold storage of calcium-treated strawberry (*Fragaria* × *ananassa* Duch.) fruit. *Postharvest Biology and Technology*, *34*, 331–339.

Lee, Y. K., & Kim, I. (2011). Modulation of fruit softening by antisense suppression of endo-beta-1,4-glucanase in strawberry. *Molecular Breeding*, *27*, 375–383.

Limpert, E., Stahel, W. A., & Abbt, M. (2001). Log-normal distributions across the sciences: Keys and clues. *Bioscience*, *51*, 341–352.

Mercado, J. A., Pliego-Alfaro, F., & Quesada, M. A. (2011). Fruit shelf life and potential for its genetic improvement. In M. A. Jenks, & P. J. Bebeli (Eds.), *Breeding for fruit quality* (pp. 81–104). Oxford: John Wiley & Sons, Inc.

Mohnen, D., Doong, R. L., Liljebjelke, K., Fralish, G., & Chan, J. (1996). Cell free synthesis of the pectic polysaccharide homogalacturonan. In J. Visser, & A. G. J. Voragen (Eds.), *Progress in biotechnology, Vol. 14*. Wageningen, The Netherlands: Elsevier, pp. 109–126.

Montreuil, G. S., Spik, G., Fournet, B., & Tollier, M. T. (1997). Nonenzymatic determinations of carbohydrates. *Analysis of Food Constituents*, *4*, 109–123.

Morris, V. J., Gromer, A., Kirby, A. R., Bongaerts, R. J. M., & Gunning, A. P. (2011). Using AFM and force spectroscopy to determine pectin structure and (bio) functionality. *Food Hydrocolloids*, *25*, 230–237.

Morris, V., Gunning, A., Kirby, A., Round, A., Waldron, K., & Ng, A. (1997). Atomic force microscopy of plant cell walls, plant cell wall polysaccharides and gels. *International Journal of Biological Macromolecules*, *21*, 61–66.

Odian, G. (2004). *Principles of polymerization*. New Jersey, USA: John Wiley & Sons, Inc.

Osorio, S., Castillejo, C., Quesada, M. A., Medina–Escobar, N., Brownsey, G. J., Suau, R., et al. (2008). Partial demethylation of oligogalacturonides by pectin methyl esterase 1 is required for eliciting defence responses in wild strawberry (*Fragaria vesca*). *The Plant Journal*, *54*, 43–55.

Ovodov, Y. (2009). Current views on pectin substances. *Russian Journal of Bioorganic Chemistry*, *35*, 269–284.

Quesada, M. A., Blanco-Portales, R., Posé, S., García-Gago, J. A., Jiménez-Bermúdez, S., Muñoz-Serrano, A., et al. (2009). Antisense down-regulation of the FaPG1 gene reveals an unexpected central role for polygalacturonase in strawberry fruit softening. *Plant Physiology*, *150*, 1022–1032.

Redgwell, R. J., Fischer, M., Kendal, E., & MacRae, E. A. (1997b). Galactose loss and fruit ripening: High-molecular-weight arabinogalactans in the pectic polysaccharides of fruit cell walls. *Planta*, *203*, 174–181.

Redgwell, R. J., MacRae, E., Hallett, I., Fischer, M., Perry, J., & Harker, R. (1997a). In vivo and in vitro swelling of cell walls during fruit ripening. *Planta*, *203*, 162–173.

Redgwell, R. J., Melton, L. D., & Brasch, D. J. (1992). Cell wall dissolution in ripening kiwifruit (*Actinidia deliciosa*): Solubilization of the pectic polymers. *Plant Physiology*, *98*, 71–81.

Redgwell, R. J., & Selvendran, R. R. (1986). Structural features of cell-wall polysaccharides of onion *Allium cepa*. *Carbohydrate Research*, *157*, 183–199.

Rimington, C. (1931). The carbohydrate complex of the serum proteins: Improved method for isolation and re-determination of structure. Isolation of glucosaminodimannose from proteins of ox blood. *The Biochemical Journal*, *25*, 1062–1071.

Rose, J. K. C., Hadfield, K. A., Labavitch, J. M., & Bennett, A. B. (1998). Temporal sequence of cell wall disassembly in rapidly ripening melon fruit. *Plant Physiology*, *117*, 345–361.

Rosli, H., Civello, P., & Martinez, G. (2004). Changes in cell wall composition of three *Fragaria* × *ananassa* cultivars with different softening rate during ripening. *Plant Physiology and Biochemistry*, *42*, 823–831.

Round, A. N., MacDougall, A. J., Ring, S. G., & Morris, V. J. (1997). Unexpected branching in pectin observed by atomic force microscopy. *Carbohydrate Research*, *303*, 251–253.

Round, A. N., Rigby, N. M., MacDougall, A. J., & Morris, V. J. (2010). A new view of pectin structure revealed by acid hydrolysis and atomic force microscopy. *Carbohydrate Research*, *345*, 487–497.

Round, A. N., Rigby, N. M., MacDougall, A. J., Ring, S. G., & Morris, V. J. (2001). Investigating the nature of branching in pectin by atomic force microscopy and carbohydrate analysis. *Carbohydrate Research*, *331*, 337–342.

Santiago-Doménech, N., Jiménez-Bemúdez, S., Matas, A. J., Rose, J. K. C., Muñoz-Blanco, J., Mercado, J. A., et al. (2008). Antisense inhibition of a pectate lyase gene supports a role for pectin depolymerization in strawberry fruit softening. *Journal of Experimental Botany*, *59*, 2769–2779.

Selvendran, R. R. (1985). Developments in the chemistry and biochemistry of pectic and hemicellulosic polymers. *Journal of Cell Science.Supplement*, *2*, 51–88.

Sene, C. F. B., McCann, M. C., Wilson, R. H., & Grinter, R. (1994). Fourier-transform Raman and Fourier-transform infrared spectroscopy (an investigation of five higher plant cell walls and their components). *Plant Physiology*, *106*, 1623–1631.

Strick, T. R., Allemand, J., Bensimon, D., Bensimon, A., & Croquette, V. (1996). The elasticity of a single supercoiled DNA molecule. *Science*, *271*, 1835–1837.

Tillmans, J., & Philippi, K. (1929). The carbohydrate content of the important proteins of foodstuffs and a colorimetric procedure for the determination of nitrogen-free sugar in protein. *Biochemische Zeitschrift*, *215*, 36–60.

Vincken, J., Schols, H. A., Oomen, R. J. F. J., McCann, M. C., Ulvskov, P., Voragen, A. G. J., et al. (2003). If homogalacturonan were a side chain of rhamnogalacturonan. I. Implications for cell wall architecture. *Plant Physiology*, *132*, 1781–1789.

Voragen, A., Coenen, G., Verhoef, R., & Schols, H. (2009). Pectin, a versatile polysaccharide present in plant cell walls. *Structural Chemistry*, *20*, 263–275.

Walkinshaw, M. D., & Arnott, S. (1981). Conformations and interactions of pectins. I. X-ray diffraction analyses of sodium pectate in neutral and acidified forms. *Journal of Molecular Biology*, *153*, 1055–1073.

Wellner, N., Kacuráková, M., Malovíková, A., Wilson, R. H., & Belton, P. S. (1998). FT-IR study of pectate and pectinate gels formed by divalent cations. *Carbohydrate Research*, *308*, 123–131.

Willats, W. G. T., Knox, J. P., & Mikkelsen, J. D. (2006). Pectin: New insights into an old polymer are starting to gel. *Trends in Food Science & Technology*, *17*, 97–104.

Willats, W. G. T., McCartney, L., Mackie, W., & Knox, J. P. (2001). Pectin: Cell biology and prospects for functional analysis. *Plant Molecular Biology*, *47*, 9–27.

Yang, H., Chen, F., An, H., & Lai, S. (2009). Comparative studies on nanostructures of three kinds of pectins in two peach cultivars using atomic force microscopy. *Postharvest Biology and Technology*, *51*, 391–398.